

Boson-fermion duality and metastability in cuprate superconductorsJ. Ranninger¹ and T. Domański²¹*Institut Néel, CNRS et Université Joseph Fourier, BP 166, 38042 Grenoble Cedex 09, France*²*Institute of Physics, Marie Curie-Skłodowska University, 20-031 Lublin, Poland*

(Received 6 November 2009; published 19 January 2010)

The intrinsic structural metastability in cuprate high- T_c materials, evidenced in a checkerboard domain structure of the CuO_2 planes, locally breaks translational and rotational symmetry. Dynamical charge-deformation fluctuations of such nanosize unidirectional domains, involving Cu-O-Cu molecular bonds, result in resonantly fluctuating diamagnetic pairs embedded in a correlated Fermi liquid. As a consequence, the single-particle spectral properties acquire simultaneously (i) fermionic low-energy Bogoliubov branches for propagating Cooper pairs and (ii) bosonic localized glassy structures for tightly bound states of them at high energies. The partial localization of the single-particle excitations leads to a fractionation of the Fermi surface as the strength of the exchange coupling between itinerant fermions and partially localized fermion pairs increases upon moving from the nodal to the antinodal point. This is also the reason why bound fermion pairs accumulate near the antinodal points and thereby control the doping dependence of the cuprates upon approaching the singular universal optimal doping rate.

DOI: [10.1103/PhysRevB.81.014514](https://doi.org/10.1103/PhysRevB.81.014514)

PACS number(s): 74.20.Mn, 74.40.-n, 74.72.-h

I. INTRODUCTION

High- T_c superconductivity of the cuprates, it is generally agreed upon, emerges out of an unconventional normal state. The most remarkable signatures of its strange metal behavior are the pseudogap in the density of states and the associated to it remnant Bogoliubov modes. Both show up in a wide temperature regime above T_c in the single-particle excitations, observed in angle-resolved photoemission spectroscopy (ARPES).¹ Novel scanning tunneling microscopy are now able to measure the spatial distribution of quasiparticle excitations on the atomic length scale²⁻⁶ and find intrinsic textured electronic structures, ranging over a wide regime from low doped to optimally doped and beyond. The spatial patterns of the single-particle spectral properties indicate an inter-relation between the low-frequency Bogoliubov modes and their high-frequency counterparts, representing localized glassy states. In this work we show how this feature can be related to a scenario in which itinerant fermionic charge carriers scatter in and out of bosonic tightly bound pairs of them in which they are momentarily trapped on nanosize deformable domains. The single-particle excitations thus appear as superpositions of itinerant and localized entities.

Ever since the discovery of the high- T_c cuprates, experimental evidence for their very unusual lattice properties has become increasingly evident. Apart from their well-established strongly correlated nature, these compounds are metastable single-phase materials.⁷ Their metastability arises from frozen-in structural misfits, involving an incompatibility between the Cu-O distances of square planar $[\text{Cu-O}_4]$ configurations in the CuO_2 planes and of cation-ligand distances in the adjacent layers. Metastable compounds have been known for a long time for their intrinsic local diamagnetic fluctuations,⁸ capable of inducing a strong pairing component in the many-body ground-state wave function. The interest in synthesizing such materials was to bypass the stringent conditions on the upper limit of T_c , imposed by phonon-mediated BCS superconductivity.⁹

On a microscopic level, the metastability in the cuprates arises from fluctuating $[\text{Cu-O-Cu}]$ molecular bonds in the CuO_2 planes.^{2,3} Their deformable ligand environments^{10,11} act as potential pairing centers⁴ for dopant holes on nanosize domains. These domains exhibit an atomic structure,⁵ which locally breaks translational as well as rotational symmetry.⁶ Two-degenerate spatially orthogonally oriented $[\text{Cu-O-Cu}]$ bonds cause the CuO_2 plane structure to segregate into a patchwork of orientationally disordered domains, separated by a lattice of essentially undeformable molecular clusters. Ultimately, this forms an effective bipartite lattice structure^{2,6} of the CuO_2 planes. The charge transfer between the pairing domains and the molecular clusters on the lattice surrounding them leads to resonant pairing on that latter. It is controlled by an interplay between localization of the charge carriers in form of bound pairs on the pairing domains and their delocalization on the lattice which spatially separates those pairing domains. On a macroscopic level, those materials exhibit an overall homogeneous crystal structure in a coarse grained sense.¹² But occasionally, such as in $\text{La}_{2-x}\text{Ba}_x\text{CuO}_4$ for $x=1/8$, the local lattice deformations of the pairing domains can lock together in a charge-ordered phase and thereby impeach superconductivity to occur.⁵

II. SCENARIO

The “formal chemical” Cu valence (not to be confused with its ionic charge) in the d -hole doped CuO_2 planes lies between Cu^{II} and Cu^{III} . For an isolated undoped CuO_2 plane this would correspond to stereochemical $[\text{Cu-O}]$ distances of 1.94 Å in the $[\text{Cu}^{\text{II}}\text{-O}_4]$ basic blocks. The misfits between the atomic structure of the CuO_2 planes and those of the adjacent layers, which furnish the dopant holes, push the bridging oxygen of the $[\text{Cu-O-Cu}]$ bonds out of the CuO_2 plane, making them buckled. By doing so, they can better accommodate the stereochemically assigned interatomic distance of those bonds.

The scenario for the doped cuprates, which we want to advocate in this work, is that the static displacements of the bridging oxygens, which characterize the undoped and low-doped insulating phase, become dynamic. The fluctuation of the bridging oxygens of the [Cu-O-Cu] bonds, in and out of the planes, tends to diminish the plane buckling which characterizes the undoped material. This tendency gets more and more pronounced as the doping is increased, driven by the increased covalency of the CuO_2 basal plane building blocks. It however shows a marked slowing down of this behavior as one passes through optimal doping.¹³ On a microscopic level, this implies fluctuations between kinked $[\text{Cu}^{\text{II}}\text{-O-Cu}^{\text{II}}]$ molecular bonds (characteristic for the undoped systems) and straight ones $[\text{Cu}^{\text{III}}\text{-O-Cu}^{\text{III}}]$ with an ideal stereochemical $[\text{Cu}^{\text{III}}\text{-O}]$ distances of 1.84 Å. In this process two holes get momentarily captured in the local dynamically deformable structure of the CuO_2 planes. It results in locally correlated charge-deformation fluctuations which break up the overall homogeneous structure of the cuprates into a checkerboard structure, as scanning tunneling microscopy (STM) results (Figs. 4 and 5 in Ref. 6) have shown. The net difference in length between the two different molecular bonds on such charge-deformation fluctuating checkerboard pairing domains will be reduced (i) because of the dynamical nature of these pairing fluctuations and (ii) because it involves cooperatively several of such $[\text{Cu-O-Cu}]$ bonds.

The likelihood of a segregation of a homogeneous lattice structure into polaronic domains, embedded in a non-polaronic matrix, such as advocated in the present scenario, had been speculated upon for a long time. For the case of intermediate electron-lattice coupling and the adiabatic to anti-adiabatic crossover regime, individual itinerant charge carriers are known to fluctuate in and out of localized polaronic states.¹⁴ Unfortunately, the present state of art of the theory of many-polaronic systems can still not handle situations other than for homogeneous or globally symmetry-broken solutions. Nevertheless indications for resonant pairing in such systems exist, where the single-particle spectral function has both coherent delocalized contributions and localized ones in form of localized polarons, respectively, bipolarons. This has been discussed in the framework of dynamical mean-field theory, numerical renormalization group, and Monte Carlo studies.¹⁵

Given the complexity of the inter-related charge-deformation dynamics in such systems, it appeared judicious to introduce a phenomenological boson-fermion model (BFM), to capture the salient features of such intrinsically locally dynamically unstable systems with a tendency to segregate into subsystems of localized and itinerant charge carriers. This idea was originally proposed by one of us (J.R.) in early 1980s in an attempt to describe the abrupt crossover between a weak-coupling adiabatic electron-phonon-mediated BCS superconductor and an insulating state, respectively, superconducting phase, of bipolarons in the strong-coupling antiadiabatic regime. The essential features of this conjectured BFM was to introduce an effective local boson-fermion exchange coupling between polaronically bound pairs and itinerant charge carriers. This picture has been substantiated subsequently by small cluster calculations for electrons strongly coupled to localized lattice vibrational

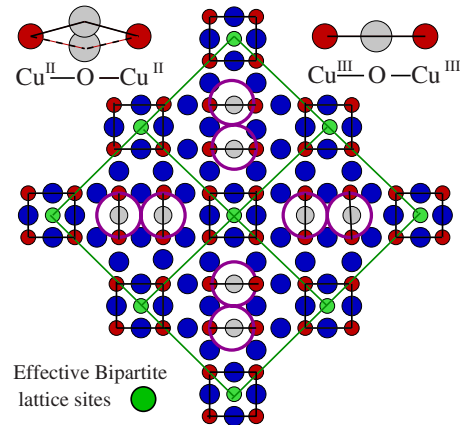


FIG. 1. (Color online) An idealized picture of the local structure of the CuO_2 planes compatible with the STM results (Refs. 2–6). It is composed of (i) Cu_4O_{12} domains acting as localizing pairing centers with directionally oriented Cu-O-Cu molecular bonds, having central bridging O's (gray circles) which can be displaced out of the CuO_2 plane and (ii) Cu_4O_4 square plaquettes housing the delocalized charge carriers. Small red circles denote Cu cations and the larger blue ones the O anions not directly involved in displacements.

modes.¹⁸ It permits to relate the effective boson-fermion exchange coupling back to the parameters, characterizing the electron-lattice coupled system, i.e., local phonon frequency and electron-phonon coupling.

In order to cast into a tractable model the physics of dynamically fluctuating $[\text{Cu-O-Cu}]$ bonds, which trigger local double charge fluctuations, we present in Fig. 1 an idealized structure for such a local checkerboard bipartite lattice structure, which comes very close to the actually observed structure. The corresponding checkerboard pairing centers consist of Cu_4O_{12} domains (three nearest-neighbor Cu-Cu distances across) on which charge carriers pair up, driven by polaronic effects. The lattice deformations of adjacent Cu_4O_{12} domains are assumed to be uncorrelated in order to prevent the system to undergo a global lattice instability. The orientational randomness of the $[\text{Cu-O-Cu}]$ unidirectional bonds, together with the quadratic Cu_4O_4 plaquettes (see Fig. 1), which separate those polaronic Cu_4O_{12} domains, justifies that. Ultimately, this results in the picture of an overall bipartite lattice structure for the CuO_2 planes with a periodicity of four nearest-neighbor Cu-Cu distances. d holes on the non-polaronic Cu_4O_4 plaquettes in the cuprates are known to behave as delocalized, though strongly correlated, entities subject to $d_{x^2-y^2}$ -wave pairing correlations.^{16,17} In the present study we shall concentrate on the purely lattice-driven pairing aspects in the cuprates, caused by their intrinsic metastabilities. We hence neglect here any Hubbard-type correlations leading to hole pairing and treat the Cu_4O_4 square plaquettes as effective lattice sites on which the charge carriers behave as itinerant uncorrelated quasiparticles. When they hop on and off the neighboring four Cu_4O_{12} pairing domains, they interact with their local dynamical deformations. To describe this effect in a tractable way, we represent the pairing domains by a single deformable molecular site on which the charge carriers pair up due to a polaronic binding mechanism. The

resulting local resonant pairing for such a setup and its manifestations in the electronic and phononic spectral properties have been studied in some detail by exact diagonalization studies.¹⁸

Indications for resonant pairing in the cuprates, driven by local dynamical lattice fluctuations can be found in quite a variety of experimental studies: the longitudinal-optical (LO) Cu-O bond-stretching mode of about 60 meV appears to be strongly coupled to charge carriers near the *hotspot* antinodal points in the Brillouin zone (BZ) $[q_x, q_y] = [\pm \pi/2, 0]$, $[0, \pm \pi/2]$.^{10,11} Their pairing results in the pseudogap feature, setting in when reducing the temperature T to below a certain strongly doping-dependent T^* . Upon entering the superconducting doping regime, coming from the insulating parent compound, this LO mode splits into two modes, separated by ≈ 10 meV.¹⁹ This indicates a crystal-lattice symmetry breaking, linked to dynamical charge inhomogeneities which are absent in the underdoped and overdoped insulating phases. Pressure,²⁰ isotope substitution studies²¹ and atomic resolution d^2I/dV^2 spectroscopy¹¹ show concomitant anticorrelated modulations of the pseudogap size and the frequency of this LO buckling mode. Correlated charge-deformation fluctuations, related to a resonant pairing superconducting phase show up in the onset of a macroscopic superfluid state of the charge carriers together with changes in the local lattice dynamics which acquires phase-correlated macroscopic features. They are seen in Rutherford backscattering experiments,²² an abrupt decrease in the kinetic energy of local vibrational modes,²³ a similar abrupt increase in a low-energy electronic background, seen in near IR excited Raman scattering²⁴ and an increase in intensity of certain Raman-active phonon modes,²⁵ indicative of changes in the scattering mechanism involving the charge carriers and local lattice modes.

III. MODEL

Superconductivity in the cuprates is destroyed, exclusively, by phase fluctuations of a bosonic order parameter^{26,27} with the finite amplitude of it, being already established well above T_c . It reflects the local nature of the Cooper pairs, whose signature is (i) a T_c scaling with the zero-temperature density of superfluid carriers²⁸ and (ii) the XY character of the transition.²⁹ The inter-relation between phase and amplitude fluctuations causes the appearance of bosonic phase modes, corresponding to propagating Cooperons, whose spectrum falls inside the gap of the fermionic single-particle excitations. Going into the normal state, above T_c , the propagating Cooperons become diffusive and the superconducting gap changes into a pseudogap in a continuous fashion.³⁰ The observed Nernst,³¹ transient Meissner effect³² and the proximity induced pseudogap³³ bare this out. The gap in the single-particle spectrum and the propagating strongly bound Cooper pairs testify the competition between amplitude and phase fluctuations of the order parameter in form of an anticorrelated T_c versus T^* variation upon changing the hole doping.^{34,35} The insulating, not antiferromagnetically ordered glassy state, at low temperature and low doping can be envisaged as a Mott correlation driven state of phase uncorre-

lated *singlet-bonding pairs*. With increased doping, this insulating state changes into a superconducting phase correlated state of such *bonding pairs*.^{36,37} Bonding pairs are defined by local linear superpositions of bound pairs and pairs of itinerant charge carriers. To what extent such an insulating state could result from a Cooper-pair Wigner crystallization, has been investigated.^{38,39}

The features which characterize the normal and superconducting phase of the cuprates necessitate to treat amplitude and phase fluctuations on an equal footing. This had originally also been the objective in conjecturing the BFM and to project out coexisting effective bosonic and fermionic charge excitations for systems which are at the frontier between amplitude-fluctuation-driven BCS superconductors and a phase-fluctuation-driven superfluidity of tightly bound real-space pairs. The BFM is designed to treat a single component system, where at any given moment a certain percentage of the charge carriers is locally paired and thus results in a finite bosonic amplitude. This is achieved by imposing a common chemical potential (determined by the bosonic energy level) for the fermionic and bosonic charge carriers. A charge exchange term, linking the fermionic and bosonic subsystem, then controls the inter-related dynamics between amplitude and phase fluctuations. It drives the system either to an insulating or superfluid state with corresponding superconducting, respectively, insulating, gaps being centered at the chemical potential. The opening of such gaps does not depend on any particular set of Fermi wave vectors and hence is unrelated to any global translational symmetry breaking.

The degree of anisotropy of pairing and of the charge-carrier dispersion in the CuO₂ planes monitors the relative importance of localization versus delocalization in different regions of the Brillouin zone. Near the antinodal points, strong pairing results from strong *intrabonding pair* correlations between bound hole pairs on the pairing centers and their itinerant counterparts in their immediate vicinity.¹⁸ It leads to their partial localization, which shows up in form of a pseudogap in the single-particle spectral properties and destroys the Fermi surface. As one moves toward the nodal points, $[k_x, k_y] = [\pm \pi/2, \pm \pi/2]$, along the so-called Fermi arc in the BZ (corresponding to the Fermi surface in the noninteracting system), those intrabonding pair phase correlations are weakened. The degree of localization then reduces and with it, the size of the pseudogap. At the same time, interbonding pair phase correlations between neighboring pairing domains come into play and with it superconducting phase locking. At low frequencies, this leads to Bogoliubov modes, which emerge out of localized phase uncorrelated bonding pairs.

We derive below these properties on the basis of the BFM, adapted to the specific anisotropic features of the cuprates. We represent the square plaquettes, housing the itinerant charge carriers, by some effective lattice sites on one sublattice and the surrounding neighboring pairing domains as effective sites on the other sublattice. We assume a d -wave symmetry for the exchange interaction between (i) pairs of itinerant charge carriers $c_{\mathbf{k}\sigma}^{(\dagger)}$ corresponding to the “plaquette site” states and (ii) polaronically bound pairs of them $b_{\mathbf{q}}^{(\dagger)}$, corresponding to the “pairing domain site” states. The

Hamiltonian describing such a scenario is then given by

$$H_{\text{BFM}} = H_{\text{BFM}}^0 + H_{\text{BFM}}^{\text{exch}}, \quad (1)$$

$$H_{\text{BFM}}^0 = \sum_{\mathbf{k}\sigma} (\varepsilon_{\mathbf{k}} - \mu) c_{\mathbf{k}\sigma}^\dagger c_{\mathbf{k}\sigma} + \sum_{\mathbf{q}} (E_{\mathbf{q}} - 2\mu) b_{\mathbf{q}}^\dagger b_{\mathbf{q}}, \quad (2)$$

$$H_{\text{BFM}}^{\text{exch}} = (1/\sqrt{N}) \sum_{\mathbf{k},\mathbf{q}} (g_{\mathbf{k},\mathbf{q}} b_{\mathbf{q}}^\dagger c_{\mathbf{q}-\mathbf{k},\downarrow} c_{\mathbf{k},\uparrow} + \text{H.c.}). \quad (3)$$

The anisotropy, which characterizes the electronic structure of cuprates, is contained in the standard expression for the bare charge-carrier dispersion given by $\varepsilon_{\mathbf{k}} = -2t[\cos k_x + \cos k_y] + 4t' \cos k_x \cos k_y$ of the CuO_2 planes with $t'/t = 0.4$ and the bare d -wave exchange coupling $g_{\mathbf{k},\mathbf{q}} = g[\cos k_x - \cos k_y]$. Given the polaronic origin of the localized pairs of tightly bound charge carriers, we assume them as dispersionless bosonic excitations with $E_{\mathbf{q}} = 2\Delta$.

The charge exchange term $H_{\text{BFM}}^{\text{exch}}$ controls the transfer of electrons (holes) between real and momentum space⁴⁰ and monitors the interplay between the delocalizing and the localizing effect. Depending on the strength of the exchange coupling $g_{\mathbf{k},\mathbf{q}}$, it results in a competition between local intrabonding pair correlations, favoring insulating features, and spatial interbonding pair correlations, favoring superconducting phase locking.³⁶ The fermionic particles thereby acquire contributions coming from the bosonic particles and the bosonic particles having features derived from their fermionic constituents. As we shall see below, the physically meaningful fermions in such a system are superpositions of fermions and bosonic bound fermion pairs, accompanied by fermion holes. This boson-fermion duality, which characterizes the electronic state of the cuprates, results from the “duplicitous”⁴⁰ nature of their charge carriers, which supports simultaneously superconducting correlations in momentum space (fermionic Bogoliubov excitations) and real-space correlations resulting in the pseudogap (derived from localized bosonic bound fermion pairs). This apparent “schizophrenic” behavior⁴¹ of the quasiparticles can be traced back to their different energy scales characterizing their excitations. Large excitation energies (above the Fermi energy) characterize their localized self-trapped nature and small excitation energies (below the Fermi energy) their quasiscoherently propagating Cooper-pair nature.

In order to obtain the spectroscopic features of effective fermionic and bosonic excitations we have to reformulate this interacting boson-fermion mixture in terms of two effective commuting Hamiltonians, one describing purely fermionic excitations and one purely bosonic ones. The boson-fermion interaction thereby is absorbed into interdependent coupling constants by renormalizing $g_{\mathbf{k},\mathbf{q}}$ down to zero via a flow-equation renormalization approach.⁴² At every step of this procedure the renormalized Hamiltonian is projected onto the basic structure given by H_{BFM}^0 plus a renormalization generated fermion-fermion interactions term⁴³

$$H_{\text{BFM}}^{F-F} = \frac{1}{N} \sum_{\mathbf{p},\mathbf{k},\mathbf{q}} U_{\mathbf{p},\mathbf{k},\mathbf{q}}^{F-F} c_{\mathbf{p}\downarrow}^\dagger c_{\mathbf{k}\downarrow}^\dagger c_{\mathbf{q}\downarrow} c_{\mathbf{p}+\mathbf{k}-\mathbf{q}\uparrow}. \quad (4)$$

This is achieved by transforming the Hamiltonian in infinitesimal steps, controlled by a flow parameter ℓ in terms of repeated unitary transformations $H(\ell) = e^{S(\ell)} H e^{-S(\ell)}$, resulting in differential equations $\partial_\ell H(\ell) = [\eta(\ell), H(\ell)]$ with $\eta(\ell) \equiv (\partial_\ell e^{S(\ell)} / \partial_\ell) e^{-S(\ell)}$, determining the flow of the parameters of our system. In its canonical form,⁴² $\eta(\ell) = [H_0(\ell), H(\ell)]$ and presents an anti-Hermitian generator. For details of the ensuing coupled nonlinear differential equations for the various ℓ -dependent parameters $\varepsilon_{\mathbf{k}}(\ell), E_{\mathbf{q}}(\ell), U_{\mathbf{p},\mathbf{k},\mathbf{q}}^{F-F}(\ell), g_{\mathbf{k},\mathbf{q}}(\ell), \mu(\ell)$ we refer the reader to our previous work.^{43,44} The parameters, characterizing H^0 and H_{exch} , evolve as the flow parameter ℓ increases. The renormalization procedure starts with $\ell=0$, for which they are given by the bare values $\varepsilon_{\mathbf{k}}, E_{\mathbf{q}} = 2\Delta, g_{\mathbf{k},\mathbf{q}}$ together with $U_{\mathbf{p},\mathbf{k},\mathbf{q}}^{F-F} \equiv 0$. The chemical potential $\mu(\ell)$ is chosen at each step of the renormalization flow such as to fix a given total number of fermions and bosons. The flow of these parameters converges for $\ell \rightarrow \infty$ and results in two uncoupled systems: one for the effective fermionic excitations and one for the effective bosonic ones with a fix point fermion dispersion $\varepsilon_{\mathbf{k}}^* = \varepsilon_{\mathbf{k}}(\ell \rightarrow \infty)$. For isotropic exchange coupling and fermion dispersion this problem had been studied previously,^{37,43,44} predicting the pseudogap⁴⁵ and damped Bogoliubov modes⁴⁴ in angle-resolved photoemission spectra. Both have since been verified experimentally.¹

IV. BOSON-FERMION DUALITY

The anisotropy of the electronic structure of cuprates tracks a changeover from self-trapped (localized) fermions, in form of diffusively propagating bosonic pairs, into itinerant propagating (delocalized) fermions upon going from the antinodal to the nodal point on an arc in the Brillouin zone, determined by $\varepsilon_{\mathbf{k}_F}^*(\phi) = \mu$. To illustrate that, we evaluate the single-particle spectral function for wave vectors $\mathbf{k} = |\mathbf{k}|[\sin \phi, \cos \phi]$, orthogonally intersecting this arc at various $\mathbf{k}_F(\phi)$, where the motion of the charge carriers is essentially one dimensional. ϕ denotes the angle of those \mathbf{k} vectors with respect to the line $[\pi, \pi] - [\pi, 0]$, (see Fig. 3).

In order to relate our study to a nearly half-filled band situation, characterizing the doped cuprates, we choose $\Delta \approx 0.75$ (in units of a nominal fermionic bandwidth of $8t$), with the bosonic level lying just barely below the center of the itinerant fermion band such as to reproduce the typical shape of the CuO_2 planar Fermi surface. For our choice of the boson-fermion exchange coupling strength $g=0.1$, which reproduces a typical onset temperature $T^* = 0.016$ for the pseudogap of roughly 100°K . For a characteristic temperature of the pseudogap phase ($T = 0.007 < T^*$), it implies a concentration of itinerant fermionic charge carriers $n_F = \sum_{\mathbf{k}\sigma} \langle c_{\mathbf{k}\sigma}^\dagger c_{\mathbf{k}\sigma} \rangle = 0.88$ and that of self-trapped ones bound into fermion pairs, $n_B = \sum_{\mathbf{q}} \langle b_{\mathbf{q}}^\dagger b_{\mathbf{q}} \rangle = 0.075$. This corresponds to a hole doping $n_h = 0.12$ with a total number of carriers of $n_{\text{tot}} = n_F + 2n_B = 1.03$. Hole doping in such a context implies a redistribution of the relative occupation of fermions and bosons and a related to it a shrinking of the arcs (see Sec. V).

The charge carriers around the nodal point turn out to be primarily given by delocalized fermionic one-particle states, while at the hotspot antinodal points they are given by localized bosonic bound fermion pairs, but which, as we shall see below, will become itinerant and eventually condense as the temperature is decreased. This is because the bare exchange coupling $g_{\mathbf{k},\mathbf{q}}$ is equal to zero at the nodal point ($\phi = \pi/4$) and increases as one moves to the antinodal points ($\phi = 0, \pi/2$), where it reaches its maximal value, equal to g . As a consequence, $\varepsilon_{\mathbf{k}}^*$ remains essentially unrenormalized for \mathbf{k} vectors crossing the arc near the nodal point. Upon approaching the antinodal point, on the contrary, $\varepsilon_{\mathbf{k}}^*$ acquires a sharp S -like inflexion at $\mathbf{k}_F(\phi)$, which leads to the appearance of the pseudogap in the single-particle density of states.

Our prime objective in the present study is to disentangle the contributions to the single-particle spectral function coming from the itinerant and from the localized features. The latter arise from single particles being momentarily trapped in form of localized pairs. The effective fermionic and bosonic excitations are obtained in a renormalization procedure similar to that of the Hamiltonian but this time by applying it to the fermion and boson operators themselves.^{44,46} The evaluation of the single-particle spectral function

$$A^F(\mathbf{k}, \omega) = -\frac{1}{\pi} \text{Im} \int_0^\beta d\tau G^F(\mathbf{k}, \tau) e^{(\omega + 0^+) \tau},$$

$$G^F(\mathbf{k}, \tau) = \langle \langle c_{\mathbf{k}\uparrow}(\tau); c_{\mathbf{k}\downarrow}^\dagger \rangle \rangle_H \quad (5)$$

in a correspondingly renormalized manner is achieved by applying the unitary transformation $e^{S(\ell)}$ to the Green's function itself. It results in

$$\begin{aligned} & \langle \langle c_{\mathbf{k}\sigma}(\tau); c_{\mathbf{k}\sigma}^\dagger(0) \rangle \rangle_H \\ &= \langle \langle e^{S(\ell)} e^{\tau H(\ell)} c_{\mathbf{k}\sigma} e^{-\tau H(\ell)} e^{-S(\ell)}; e^{S(\ell)} c_{\mathbf{k}\sigma}^\dagger e^{-S(\ell)} \rangle \rangle_{H(\ell)} \\ &= \langle \langle e^{S(\infty)} e^{\tau H^*} c_{\mathbf{k}\sigma} e^{-\tau H^*} e^{-S(\infty)}; e^{S(\infty)} c_{\mathbf{k}\sigma}^\dagger e^{-S(\infty)} \rangle \rangle_{H^*}, \end{aligned} \quad (6)$$

where the trace has to be carried out over the fully renormalized fixed point Hamiltonian H^* . Neglecting the residual interaction $U_{\mathbf{p},\mathbf{k},\mathbf{q}}^{F-F}$ between the fermions and restricting ourselves to the pseudogap phase without any long-range phase locking, we obtain the following renormalized fermion operators⁴⁶

$$\begin{bmatrix} c_{-\mathbf{k},-\sigma}^\dagger(\ell) \\ c_{\mathbf{k},\sigma}(\ell) \end{bmatrix} = u_{\mathbf{k}}^F(\ell) \begin{bmatrix} c_{-\mathbf{k},-\sigma}^\dagger \\ c_{\mathbf{k},\sigma} \end{bmatrix} \mp \frac{1}{\sqrt{N}} \sum_{\mathbf{q}} v_{\mathbf{k},\mathbf{q}}^F(\ell) \begin{bmatrix} b_{\mathbf{q}}^\dagger c_{\mathbf{q}+\mathbf{k},\sigma} \\ b_{\mathbf{q}} c_{\mathbf{q}-\mathbf{k},-\sigma}^\dagger \end{bmatrix}, \quad (7)$$

with ℓ -dependent parameters $u_{\mathbf{k}}^F(\ell), v_{\mathbf{k},\mathbf{q}}^F(\ell)$ determined by the flow equations. The single-particle fermionic spectral function resulting from such a procedure

$$A^F(\mathbf{k}, \omega) = |u_{\mathbf{k}}^F(\infty)|^2 \delta(\omega + \mu - \varepsilon_{\mathbf{k}}^*) + \frac{1}{N} \sum_{\mathbf{q} \neq 0} (n_{\mathbf{q}}^B + n_{\mathbf{q}-\mathbf{k}}^F) \times |v_{\mathbf{k},\mathbf{q}}^F(\infty)|^2 \delta(\omega - \mu + \varepsilon_{\mathbf{q}-\mathbf{k}}^* - E_{\mathbf{q}}^*), \quad (8)$$

is illustrated in Fig. 2 for $T=0.007$ ($< T^*=0.016$), which lies in the pseudogap phase. We choose a \mathbf{k} traversing the arc in the Brillouin zone at $\mathbf{k}_F(\phi)$, in a characteristic region around

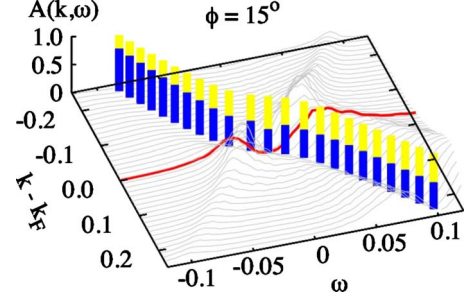


FIG. 2. (Color online) $A(\mathbf{k}, \omega)$ at $T=0.007$ ($< T^*=0.016$) as a function of $|\mathbf{k}|$ (in units of the inverse lattice vector) near \mathbf{k}_F (red line), corresponding to $\phi=15^\circ$, orthogonally crossing the Fermi arc. The spectral weight of the coherent and incoherent contributions are indicated by blue (bottom part) and yellow (top part) bars, respectively.

$\phi = \phi_c = 15^\circ$, where the T -independent gap for $\phi \leq \phi_c$ changes over into a T -dependent gap in the single-particle density of states for values of $\phi \geq \phi_c$ (see Fig. 3). ϕ_c signals the separation between localized and delocalized, respectively, bosonic and fermionic, features in the Brillouin zone.

For \mathbf{k} vectors below $\mathbf{k}_F(\phi)$, $A^F(\mathbf{k}, \omega)$ exhibits (i) low-energy ($\leq \mu$) delocalized single-particle excitations [the first term in Eq. (8)], which follow essentially the dispersion $\varepsilon_{\mathbf{k}}^* \simeq \varepsilon_{\mathbf{k}}$ and (ii) a high-energy ($\geq \mu$) broadened upper Bogoliubov branch. For $k \rightarrow 0$ that latter merges into the time-reversed spectrum $-\varepsilon_{\mathbf{k}}$. For wave vectors \mathbf{k} above $\mathbf{k}_F(\phi)$, $A^F(\mathbf{k}, \omega)$ shows simultaneously two features: (i) low-frequency diffusively propagating Bogoliubov modes and (ii) high-frequency single-particle excitations with a dispersion given by $\varepsilon_{\mathbf{k}}^* \simeq \varepsilon_{\mathbf{k}}$ and moving in a cloud of bosonic two-particle excitations in form of bonding and antibonding states, seen by the wings on either side of the coherent part [the first term in Eq. (8)] of those excitations. These low- and high-frequency excitations for a given wave vector characterize the low- and high-frequency response of one and the same phenomenon, with the latter testing the internal degrees of freedom of the collective diffusively propagating Bogoliubov modes. These internal degrees of freedom are images of localized bonding and antibonding states, such as given by the Green's function in the atomic limit ($t, t'=0$),^{47,48} $G_{at}^F(i\omega_n) = 1/[G_{at}^F(i\omega_n)^{-1} - \Sigma_{at}^F(i\omega_n)]$ with the self-energy

$$\Sigma_{at}^F(i\omega_n) = \frac{(1-Z)g^2(i\omega_n + \mu)}{[(i\omega_n + \mu)(i\omega_n - 2\Delta + \mu) - Zg^2]}, \quad (9)$$

having, apart from a characteristic BCS-type structure for localized Cooper pairs, a substantial contribution from in-

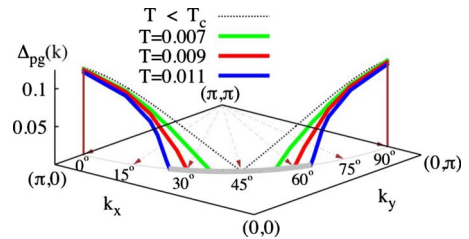


FIG. 3. (Color online) Variation in the pseudogap for different k vectors, orthogonally crossing the arc, given by angles ϕ . With increasing T , Δ_{pg} tend to zero at smaller and smaller values of ϕ .

gap single-particle states. They are a hallmark of the non-BCS physics involved here and expected to show up in sufficiently refined ARPES studies. $Z \approx 2/[3 + \cosh(g/k_B T)]$ (for our choice of parameters) denotes the spectral weight of non-bonding delocalized charge carriers, described by $G_0^F(i\omega_n) = 1/(i\omega_n - \mu)$.

A pseudogap in the density of states, $\rho(\omega) = (1/N)\sum_{\mathbf{k}} A^F(\mathbf{k}, \omega)$ opens up at some $T = T^*$ at $\mathbf{k}_F(\phi)$. Its size, $\Delta_{pg}(\phi)$, is determined by the distance between the peaks either side of $\varepsilon_{\mathbf{k}_F(\phi)}^*$, when upon lowering T the deviation from the bare density of state, $\rho^0(\omega) = (1/N)\sum_{\mathbf{k}} \delta(\omega - \varepsilon_{\mathbf{k}})$ becomes noticeable. We take as a criterion a reduction to 90% of $\rho^0(\omega=0)$. The sharp peak in $A^F(\mathbf{k}_F, \omega)$ in Fig. 2, arising from the coherent part of this spectrum, is a consequence of having neglected the residual fermion-fermion interaction $U_{\mathbf{p},\mathbf{k},\mathbf{q}}^{F-F}$, Eq. (4). The effect of this interaction is to broaden this delta-functionlike peak, as we know from previous studies using different approaches.^{49,50} To describe this effect within the present flow equation approach, requires a fully self-consistent treatment of the diagonal part of the renormalized fermions given by $\sum_{\mathbf{k}\sigma} (\varepsilon_{\mathbf{k}}^* - \mu) c_{\mathbf{k}\sigma}^\dagger c_{\mathbf{k}\sigma}$ and the residual fermion-fermion interaction H_{BFM}^{F-F} , an issue, which will be treated in some future study.

The appearance of the pseudogap is associated with a reduction in the spectral weight of this coherent contribution (given by the height of the blue bottom part bars in Fig. 2). We illustrate in Fig. 3 the variation in $\Delta_{pg}(\phi)$ for different T . Close to the antinodal point, the localized and bosonic dominated regime, it is relatively T independent. But approaching the nodal point, it abruptly drops to zero, even though $g_{\mathbf{k},\mathbf{q}}$ is still finite. Although reminiscent of BCS-type superconducting correlations (without any pseudogap) for $60^\circ \geq \phi \geq 30^\circ$, the momentum dependence of the gap in the superconducting phase is T dependent and thus speaks against any BCS mean-field-type behavior.⁵¹ The reason behind the change-over from an essentially T -independent gap for $\phi \leq \phi_c$ and a T -dependent gap for $\phi \geq \phi_c$ is the following: as ϕ decreases, the size of the pseudogap increases and at the same time its position in the Brillouin zone at some $\mathbf{k}_F(\phi)$ diminishes until it reaches the bottom of $\varepsilon_{\mathbf{k}}^*$. (see Fig. 2 in Ref. 37). At that point, itinerant fermionic charge carriers disappear in that part for the Brillouin zone, having been converted into bosonic-fermion pairs. The accumulation of such bosonic charge carriers near the antinodal point is a direct consequence of the anisotropic boson-fermion exchange coupling and d -wave pairing in those cuprates. Since the excitation energies (size of the pseudogap) characterizing such entities are determined by purely local effects, they are relatively temperature as well as doping independent for $\phi \leq \phi_c$. Doping dependent however is the value $\phi = \phi_c$ of the crossover to itinerant fermionic charge carriers, as confirmed in ARPES experiments.⁵¹

In order to visualize the accumulation of bosonic charge carriers near the antinodal points let us investigate how the fermionic charge carriers in the various regions near the arc in the Brillouin zone get converted into diffusively propagating bound pairs of them. To do that we evaluate the renormalized Bose spectral function,

$$A^B(\mathbf{q}, \omega) = -\frac{1}{\pi} \text{Im} \int_0^\beta d\tau G^B(\mathbf{q}, \tau) e^{(\omega + i0^+) \tau},$$

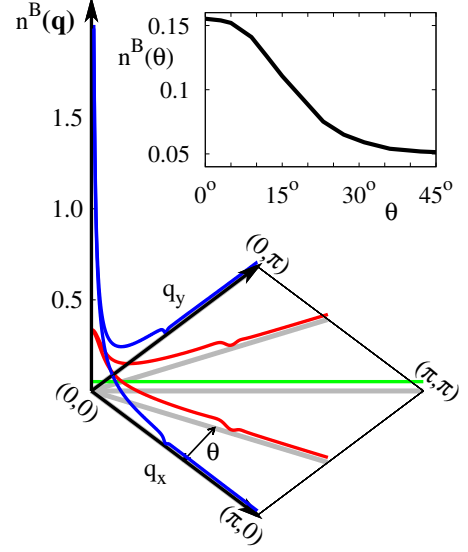


FIG. 4. (Color online) Variation in the number of paired fermions as a function of wave vectors \mathbf{q} along different directions in the Brillouin zone given by the angle θ . The variation in the total number of such pairs is illustrated in the inset.

$$G^B(\mathbf{q}, \tau) = \langle \langle b_{\mathbf{q}}(\tau); b_{\mathbf{q}}^\dagger \rangle \rangle_H, \quad (10)$$

for which we had previously derived the corresponding renormalization flow equations.⁴⁶ It results in renormalized boson operators

$$b_{\mathbf{q}}(\ell) = u_{\mathbf{q}}^B(\ell) b_{\mathbf{q}} + \frac{1}{\sqrt{N}} \sum_{\mathbf{k}} v_{\mathbf{q},\mathbf{k}}^B(\ell) c_{\mathbf{k}\downarrow} c_{\mathbf{q}-\mathbf{k}\uparrow} \quad (11)$$

with $b_{\mathbf{q}}^\dagger(\ell) = [b_{\mathbf{q}}(\ell)]^\dagger$ and which ultimately leads to the renormalized boson spectral function given by

$$A^B(\mathbf{q}, \omega) = |u_{\mathbf{q}}^B(\infty)|^2 \delta(\omega - E_{\mathbf{q}}^*) + \frac{1}{N} \sum_{\mathbf{k}} f_{\mathbf{k},\mathbf{q}-\mathbf{k}} |v_{\mathbf{q},\mathbf{k}}^B(\infty)|^2 \delta(\omega - \varepsilon_{\mathbf{k}}^* - \varepsilon_{\mathbf{q}-\mathbf{k}}^*). \quad (12)$$

The corresponding number of such bosonic charge carriers is given by $n^B(q_x, q_y) = \int d\omega A^B(\mathbf{q}, \omega) [\exp(\omega/k_B T) - 1]^{-1}$. We plot it for a series of \mathbf{q} vectors in Fig. 4 for $T=0.007$, which sample the anisotropy of the CuO_2 electronic structure, where θ indicates the azimuthal angle in this plane. Notice that along the nodal direction the number of bosons is independent on $|\mathbf{q}|$ because of the absence of any boson-fermion coupling. As one approaches the direction linking the center of the zone with the antinodal points, the exchange coupling steadily increases and consequently the intrinsically localized bosons acquire itinerancy and gather in a region of long wavelength. Those bosons have internal structure of two fermions with opposite momenta centered around $\mathbf{k}_F(\phi)$. In the inset of Fig. 4 we illustrate the total number of such bosons along the various \mathbf{q} vectors and notice the relative increase, respectively, decrease compared to their average value 0.075, depending on whether we are sampling the nodal or the antinodal directions. The accumulation of fermi-

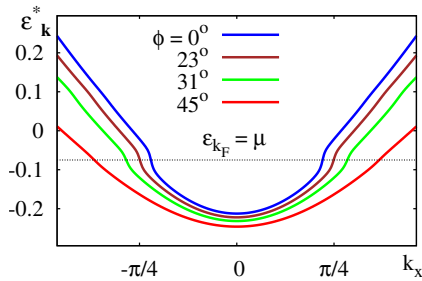


FIG. 5. (Color online) Variation in the renormalized single-particle dispersion for wave vectors \mathbf{k} orthogonally crossing the arcs along different directions in the Brillouin zone, characterized by the angle $\phi = \arcsin(k_x/|\mathbf{k}|)$. The reduction in the value of $|\mathbf{k}_F(\phi)|$ upon approaching the antinodal regime indicates an emptying out of the fermionic single-particle excitations in favor of an increase in their paired states.

ons getting converted into fermion pairs in certain parts of the Brillouin zone, close the antinodal points, has its counterpart in the diminishing density of single-particle fermionic excitations in the same regions. We illustrate that in Fig. 5, where we plot the variation in the coherent part of the single-particle dispersion, given by $\varepsilon_{\mathbf{k}}^*$ around $\mathbf{k}_F(\phi)$. We notice that with diminishing ϕ , approaching the antinodal points, the corresponding value of $\mathbf{k}_F(\phi)$ diminishes. This announces a shrinking of the Fermi sea, causing an emptying out of single-particle states and consequently an increase in bound fermion pairs. This feature had previously been observed in connection with the transition between the superconducting state of phase-correlated bonding pairs and the insulating state of such phase-uncorrelated bonding pairs.³⁷

V. SUMMARY AND OUTLOOK

The present scenario for the cuprates is based on resonant pairing induced by local dynamical lattice instabilities. It makes use of the fact that such systems are prone to segregation of globally homogeneous structures into small nanosize pairing domains, which locally break the translational as well as rotational symmetry by randomly orienting unidirectional [Cu-O-Cu] molecular bonds in different directions. This leads to fermionic charge carriers having single-particle spectral features which comprise simultaneously: (i) quasilocalized self-trapped charge carriers, which are momentarily trapped in form of bound pairs in polaronic charge fluctuating local domains and (ii) delocalized states on a sublattice in which those polaronic domains are embedded.

Due to the d -wave symmetry of pairing, which in our case is encoded in the anisotropic boson-fermion exchange coupling $g_{\mathbf{k},\mathbf{q}}$, the spectral properties of the single-particle excitations exhibit a pseudogap with the following features: as we move on a constant energy line in the Brillouin zone, corresponding to the chemical potential (where such an arc determines the Fermi surface, whenever it exists), $|g_{\mathbf{k},\mathbf{q}}|$ diminishes as we go from the antinodal ($\phi=0$) to the nodal region ($\phi=\pi/4$). For $0 < \phi < \phi_c$, with $\phi_c \approx 15^\circ$, for our choice of parameters and total carrier concentration $n_{tot} = n_F + 2n_B \approx 1$, the size of the pseudogap, Δ_{pg} , diminishes with

increasing ϕ but remains relatively unaffected by changes in temperature T . On the contrary, the single-particle excitations on that arc for $\phi_c < \phi < \pi/4$, exhibit a Δ_{pg} which, while still decreasing with increasing ϕ upon approaching the nodal region, now is strongly T dependent. For low T , Δ_{pg} remains rather robust upon increasing ϕ , tending to zero gradually as one approaches $\phi = \pi/4$. Yet, with increasing T , it tends to zero more and more rapidly at larger and larger values of ϕ , (see Fig. 3). Those features, which have been observed experimentally,⁶ suggest that: (i) the pseudogap in a finite region ($0 < \phi < \phi_c$) around the antinodal point is controlled by predominately local pairing effects (via the intrabonding mechanism), which is independent on doping and largely unaffected by superconducting phase fluctuations. (ii) The pseudogap in a finite region ($\phi_c < \phi < \pi/4$) around the nodal point is controlled by both, local intrabonding as well as the nonlocal superconducting *interbonding* correlations. The latter are sensitive to phase fluctuations and cause the dependence of Δ_{pg} on T as well as on doping.

Apart from these experimentally confirmed features, the present study demonstrates that diffusively propagating Bogoliubov excitation should be visible in ARPES also in the regions of the Brillouin-zone regime where a finite pseudogap exists, such as near the antinodal point. Given the T -independent Δ_{pg} one cannot expect any significant phase locking there. The reason for that is that the Cooperons still have a finite mobility of their center-of-mass motion over short distances for which phase locking is not required. Earlier studies, based on self-consistent diagrammatic approaches,³⁰ have shown that the carriers assuring the transport properties change gradually from fermionic to bosonic bound fermion pairs as T decreases below T^* and eventually transits the pseudogap phase into a Bose metallic/superconducting phase.³⁷ The manifestation of diffusive low-energy Bogoliubov modes for $\mathbf{k} \leq \mathbf{k}_F$ near the antinodal points are thus a signature of a prevailing glassy Bose metallic, respectively, superconducting, behavior in a restricted area of the Brillouin zone. The internal structure of those diffusively propagating Cooperons consists of self-trapped fermions. This self-trapped nature shows up in their single-particle excitations above the chemical potential. They reflect their atomic localized nature, where two-particle localized bonding and antibonding satellites trail the dispersion of their delocalized coherent part. The low-energy diffusive collective Bogoliubov excitations and the high-energy single-particle excitations are simply two different manifestations of the same entity. Whether there is a sharp border line for the onset of the high-energy localized features in the Brillouin zone, as suggested by a so-called doping independent “extinction line,”^{6,40} will have to be checked in future for the present scenario.

Let us conclude this study with some remarks on the kind of doping mechanism at play in the cuprate high- T_c compounds. For low hole doping it can be understood in terms of a doped Mott insulator and an antiferromagnetic ground state, transiting into a spin-singlet liquid glassy state with increased doping. For the remaining doping regime, approaching the optimal and overdoped regions, it remains an open problem to be resolved. Experimentally one finds a singular universal optimal doping rate $n_h^{opt} = 0.16$ holes/Cu

atom, where T_c reaches its maximum together with a maximal volume fraction of the Meissner effect and a Hall number becoming sharply peaked.⁵² In scenarios, like the present one, based on a competition between amplitude and phase fluctuations, this doping rate also characterizes the region where the energies of the superconducting phase stiffness and that of the pairing coincide.²⁶ These unusual electronic effects are accompanied by a reduction in the buckling of the CuO_2 planes, which characterize the low-doped insulating phase. It is caused by a reduction in the Cu-O bond lengths.¹³ Pressure-tuned electronic transitions, testing electronic and lattice features at the same time,⁵³ point to a critical pressure which can be identified with the critical doping rate n_h^{opt} . The universal values of n_h^{opt} , occurs for any optimally doped system, whatever its chemical structure of the doping blocks might be. This suggests that, upon approaching optimal doping, the electronic and lattice degrees of freedom get strongly locked together⁵⁴ and by doing so increase the stability of these intrinsically metastable materials. And indeed, upon forcing extra holes into such systems by overdoping $n_h > n_h^{opt}$, it appears that they segregate into different crystalline phases,⁵⁵ with superconducting components composed of underdoped and optimally doped regions. Understanding the doping dependence of the cuprates thus reduces effectively to understanding the structural stability of those system. This must involve correlated macroscopic features^{22,23} of charge and lattice deformations, such that precisely at optimal doping they optimally and constructively interfere with each other. Transposing these experimental facts on the scenario discussed in this paper, the fluctuating local domains in the CuO_2 planes get increasingly more coherently locked together as hole doping increases. This results in a decrease in spatial phase fluctuations of the bosonic resonantly bound fermion pairs driven by locally fluctuating lattice structures while at the same time their conjugate amplitude fluctuations increase. As a consequence T_c increases and T^* decreases. Previous studies^{56,57} on the interplay between amplitude and phase fluctuations bares that out. The relevant quantity in our scenario, which controls this doping dependence, is thus the strength of the phenomenological boson-fermion exchange coupling, which has to decrease upon approaching optimal doping. It is that which controls the local lattice dynamics,

fluctuating between different stereochemical configurations related to different molecular valence states and hence charges.¹⁸

According to these experimental facts, the chemical-doping mechanism which imposes itself in the cuprates, is that it converts part of the itinerant electrons into polaronically driven resonating pairs in certain regions of the Brillouin zone (see Fig. 4), manifests in the opening of a pseudogap around the so-called hotspots. The self-regulating redistribution of itinerant charge carriers and bosonic bound pairs of them on arcs in the Brillouin zone, which are images of the Fermi surface, is an intrinsic rather than an extrinsic⁵⁸ feature of the scenario presented here. It originates from strong electron-lattice coupling, in a system with a highly anisotropic electronic dispersion and coupling to local lattice modes, evidenced in the anisotropic isotope-dependent pseudogap and responsible for the local symmetry breaking of those systems. The doping-induced creation of bosonic charge carriers out of the sea of itinerant electrons, leads to a concomitant reduction in the number of the latter. This implies a shrinking of the Fermi volume (see Fig. 5), which is tantamount to the creation of holes with respect to the half-filled band situation for undoped insulating systems. Our doping scenario envisages that the total number of charge carriers, composed of bosonic-fermion pairs and itinerant fermions remains constant throughout this doping procedure. Their relative densities however vary as the boson-fermion exchange coupling increases, upon going from the stable optimally doped case toward low doping. A recent study³⁷ of the transition from a superconducting phase into an insulating bonding-pair liquid state, upon increasing this boson-fermion coupling, enforces our picture for such a doping mechanism in the cuprates. The recently observed breakdown of their homogeneous crystal structures into translational/rotational symmetry broken local clusters, discussed from a theoretical point in this paper, should trigger new ways of looking at those systems.

ACKNOWLEDGMENT

We thank Juergen Roehler for constructive remarks concerning this work and its presentation.

-
- ¹A. G. Loeser, Z.-X. Shen, D. S. Dessau, D. S. Marshall, C. H. Park, P. Fournier, and A. Kapitulnik, *Science* **273**, 325 (1996); H. Ding, T. Yokoya, J. C. Campuzano, T. Takahashi, M. Randeria, M. R. Norman, T. Mochiku, K. Kadowaki, and J. Giapintzakis, *Nature (London)* **382**, 51 (1996); A. Kanigel, U. Chatterjee, M. Randeria, M. R. Norman, G. Koren, K. Kadowaki, and J. C. Campuzano, *Phys. Rev. Lett.* **101**, 137002 (2008).
- ²Y. Kohsaka, C. Taylor, K. Fujita, A. Schmidt, C. Lupien, T. Hanaguri, M. Azuma, M. Takano, H. Eisaki, H. Takagi, S. Uchida, and J. C. Davis, *Science* **315**, 1380 (2007).
- ³K. K. Gomes, A. N. Pasupathy, A. Pushp, S. Ono, Y. Ando, and A. Yazdani, *Nature (London)* **447**, 569 (2007).
- ⁴K. McElroy, R. W. Simmonds, J. E. Hoffman, D.-H. Lee,

- J. Orenstein, H. Eisaki, S. Uchida, and J. C. Davis, *Nature (London)* **422**, 592 (2003).
- ⁵T. Valla, A. V. Fedorov, J. Lee, J. C. Davis, and G. D. Gu, *Science* **314**, 1914 (2006).
- ⁶Y. Kohsaka, C. Taylor, P. Wahl, A. Schmidt, J. Lee, K. Fujita, J. W. Alldredge, K. McElroy, J. Lee, H. Eisaki, S. Uchida, D.-H. Lee, and J. C. Davis, *Nature (London)* **454**, 1072 (2008).
- ⁷A. W. Sleight, *Phys. Today* **44**(6), 24 (1991).
- ⁸J. M. Vandenberg and B. T. Matthias, *Science* **198**, 194 (1977).
- ⁹P. W. Anderson and B. T. Matthias, *Science* **144**, 373 (1964).
- ¹⁰T. Cuk, F. Baumberger, D. H. Lu, N. Ingle, X. J. Zhou, H. Eisaki, N. Kaneko, Z. Hussain, T. P. Devereaux, N. Nagaosa, and Z.-X. Shen, *Phys. Rev. Lett.* **93**, 117003 (2004).

- ¹¹J. Lee, K. Fujita, K. McElroy, J. A. Slezak, M. Wang, Y. Aiura, H. Bando, M. Ishikado, T. Masui, J.-X. Zhu, A. V. Balatsky, H. Eisaki, S. Uchida, and J. C. Davis, *Nature (London)* **442**, 546 (2006).
- ¹²A. V. Balatsky and J.-X. Zhu, *Phys. Rev. B* **74**, 094517 (2006).
- ¹³J. Röhler, *Physica C* **408-410**, 458 (2004).
- ¹⁴D. M. Eagles, *Phys. Status Solidi B* **48**, 407 (1971); K. Cho and Y. J. Toyozawa, *Phys. Soc. Jap.* **30**, 1555 (1971); H. B. Shore and L. M. Sanders, *Phys. Rev. B* **7**, 4537 (1973).
- ¹⁵S. Ciuchi, M. Capone, E. Cappeluti, and G. Sangiovanni, *Proceedings of International School of Physics "Enrico Fermi," Course CLXI*, edited by G. Iadonisi, J. Ranninger and G. de Filippis (IOS, The Netherlands, 2006), p 131; A. C. Hewson, *ibid.* p. 155; A. S. Mischenko, *ibid.* p. 177.
- ¹⁶J. E. Hirsch, S. Tang, E. Loh, Jr., and D. J. Scalapino, *Phys. Rev. Lett.* **60**, 1668 (1988).
- ¹⁷E. Altman and A. Auerbach, *Phys. Rev. B* **65**, 104508 (2002).
- ¹⁸J. Ranninger and A. Romano, *Europhys. Lett.* **75**, 461 (2006); *Phys. Rev. B* **78**, 054527 (2008).
- ¹⁹D. Reznik, L. Pintschovius, M. Ito, S. Iikubo, M. Sato, H. Goka, M. Fujita, K. Yamada, G. D. Gu, and J. M. Tranquada, *Nature (London)* **440**, 1170 (2006).
- ²⁰P. S. Häfliger, A. Podlesnyak, K. Conder, and A. Furrer, *Europhys. Lett.* **73**, 260 (2006).
- ²¹D. Rubio Temprano, J. Mesot, S. Janssen, A. Furrer, K. Conder, and H. Mutka, *Phys. Rev. Lett.* **84**, 1990 (2000).
- ²²R. P. Sharma, T. Venkatesan, Z. H. Zhang, J. R. Liu, R. Chu, and W. K. Chu, *Phys. Rev. Lett.* **77**, 4624 (1996).
- ²³H. A. Mook, M. Mostoller, J. A. Harvey, N. W. Hill, B. C. Chakoumakos, and B. C. Sales, *Phys. Rev. Lett.* **65**, 2712 (1990).
- ²⁴G. Ruani and P. Ricci, *Phys. Rev. B* **55**, 93 (1997).
- ²⁵O. V. Misochko, E. Y. Sherman, N. Umesaki, K. Sakai, and S. Nakashima, *Phys. Rev. B* **59**, 11495 (1999).
- ²⁶V. J. Emery and S. A. Kivelson, *Nature (London)* **374**, 434 (1995).
- ²⁷M. Franz and A. J. Millis, *Phys. Rev. B* **58**, 14572 (1998).
- ²⁸Y. J. Uemura, G. M. Luke, B. J. Sternlieb, J. H. Brewer, J. F. Carolan, W. N. Hardy, R. Kadono, J. R. Kempton, R. F. Kiefl, S. R. Kretzmann, P. Mulhern, T. M. Riseman, D. L. Williams, B. X. Yang, S. Uchida, H. Takagi, J. Gopalakrishnan, A. W. Sleight, M. A. Subramanian, C. L. Chien, M. Z. Cieplak, G. Xiao, V. Y. Lee, B. W. Statt, C. E. Stronach, W. J. Kossler, and X. H. Yu, *Phys. Rev. Lett.* **62**, 2317 (1989).
- ²⁹M. B. Salamon, J. Shi, N. Overend, and M. A. Howson, *Phys. Rev. B* **47**, 5520 (1993).
- ³⁰P. Devillard and J. Ranninger, *Phys. Rev. Lett.* **84**, 5200 (2000).
- ³¹Y. Wang, L. Li, and N. P. Ong, *Phys. Rev. B* **73**, 024510 (2006).
- ³²J. Corson, R. Mallozzi, J. Orenstein, J. N. Eckstein, and I. Bozovic, *Nature (London)* **398**, 221 (1999).
- ³³O. Yuli, I. Asulin, Y. Kalcheim, G. Koren, and O. Millo, *Phys. Rev. Lett.* **103**, 197003 (2009).
- ³⁴Z. Tešanović, *Nat. Phys.* **4**, 408 (2008).
- ³⁵S. Hüfner, M. A. Hossain, A. Damascelli, and G. A. Sawatzky, *Rep. Prog. Phys.* **71**, 062501 (2008).
- ³⁶M. Cuoco and J. Ranninger, *Phys. Rev. B* **74**, 094511 (2006).
- ³⁷T. Stauber and J. Ranninger, *Phys. Rev. Lett.* **99**, 045301 (2007).
- ³⁸Z. Tešanović, *Phys. Rev. Lett.* **93**, 217004 (2004).
- ³⁹T. Pereg-Barnea and M. Franz, *Phys. Rev. B* **74**, 014518 (2006).
- ⁴⁰T. Hanaguri, *Nature (London)* **454**, 1062 (2008).
- ⁴¹B. Goss Levi, *Phys. Today* **60** (12)17 (2007).
- ⁴²F. Wegner, *Ann. Phys. (Leipzig)* **3**, 77 (1994).
- ⁴³T. Domanski and J. Ranninger, *Phys. Rev. B* **63**, 134505 (2001).
- ⁴⁴T. Domanski and J. Ranninger, *Phys. Rev. Lett.* **91**, 255301 (2003).
- ⁴⁵J. Ranninger, J. M. Robin, and M. Eschrig, *Phys. Rev. Lett.* **74**, 4027 (1995).
- ⁴⁶T. Domański and J. Ranninger, *Phys. Rev. B* **70**, 184503 (2004).
- ⁴⁷T. Domański, J. Ranninger and J.-M. Robin, *Solid State Commun.* **105**, 473 (1998).
- ⁴⁸T. Domański, *Eur. Phys. J. B* **33**, 41 (2003).
- ⁴⁹J. Ranninger and J.-M. Robin, *Solid State Commun.* **98**, 559 (1996).
- ⁵⁰J. M. Robin, A. Romano, and J. Ranninger, *Phys. Rev. Lett.* **81**, 2755 (1998).
- ⁵¹W. S. Lee, I. M. Vishik, K. Tanaka, D. H. Lu, T. Sasagawa, N. Nagaosa, T. P. Devereaux, Z. Hussain, and Z.-X. Shen, *Nature (London)* **450**, 81 (2007).
- ⁵²F. F. Balakirev, J. B. Betts, A. Migliori, S. Ono, Y. Ando, and G. S. Boebinger, *Nature (London)* **424**, 912 (2003).
- ⁵³T. Cuk, V. Struzhkin, T. P. Devereaux, A. Goncharov, C. Kendziora, H. Eisaki, H. Mao, and Z. X. Shen, *Phys. Rev. Lett.* **100**, 217003 (2008).
- ⁵⁴J. Roehler, *Proceedings of International Conference on Materials and Mechanisms of Superconductivity*, Tokyo, 2009 (unpublished).
- ⁵⁵V. P. Martovitsky, A. Krapf, and L. Dudy, *JETP Lett.* **85**, 292 (2007).
- ⁵⁶J. Ranninger and L. Tripodi, *Phys. Rev. B* **67**, 174521 (2003).
- ⁵⁷M. Cuoco and J. Ranninger, *Phys. Rev. B* **70**, 104509 (2004).
- ⁵⁸A. Perali, C. Castellani, C. Di Castro, M. Grilli, E. Piegari, and A. A. Varlamov, *Phys. Rev. B* **62**, R9295 (2000).